European Polymer Journal 194 (2023) 112144

Contents lists available at ScienceDirect

European Polymer Journal

journal homepage: www.elsevier.com/locate/europolj

Thermogels based on biocompatible OEGMA-MEGMA diblock copolymers

Qian Li [a], Ruiqi Wang [a], Jun Lee [a], Joana S. Correia [a], Anna P. Constantinou [a], Jonathan Krell [b], Theoni K. Georgiou [a,*]

[a] Department of Materials, Imperial College London, London, UK
[b] Department of Surgery & Cancer, Imperial College London, UK

ARTICLE INFO

Keywords:
Group transfer polymerisation
Thermoresponsive polymers
Oligo(ethylene glycol) methacrylates
Mono(ethylene glycol) methacrylate
Thermogelling
Diblock copolymers

ABSTRACT

A series of biocompatible thermoresponsive copolymers were successfully synthesised via group transfer polymerisation (GTP) from methoxy ethylene glycol methacrylate (MEGMA) and methoxy oligo (ethylene glycol) methacrylate (OEGMA, M_n = 300 g mol $^{-1}$). Statistical and diblock copolymers with molar mass around 8100 g mol^{-1} and various compositions were investigated. Specifically, the content in OEGMA and MEGMA was varied from 80 to 20, 70–30, 60–40, to 50–50 w/w%. The thermoresponsive and self-assembly behaviour of the copolymers was investigated through visual tests, rheology, dynamic light scattering (DLS) and transmission electron microscopy (TEM). Interestingly, the diblock copolymers with higher MEGMA content were able to form gels at relatively low concentrations (as low as 5% w/w) when increasing the temperature, something that is reported for the first time for linear ethylene glycol based copolymers. A transition of spherical micelle to worm-like micelle was observed in these diblock copolymers that promotes gelation. Furthermore, these in-house synthesised polymers were mixed with Pluronic® F127. It was found that the gelation area of Pluronic® F127 was broadened by the addition of the synthesised copolymers with one formulation, specifically a combination of 12.5% w/w Pluronic® F127 and 12.5% w/w of a statistical OEGMA-*co*-MEGMA, forming a stable gel from 34 °C to 48 °C that is a desirable temperature range for biological applications. Finally, cell viability experiments were performed for the three most promising diblock copolymers and they were confirmed to be non-toxic.

1. Introduction

Smart materials which can respond to external stimuli, such as temperature, pressure, light, *etc*, have drawn much attention over the past decades [1-3]. Among these smart materials, thermoresponsive hydrogels are of great interest in biomedical applications, such as injectable gel [4-6], tissue engineering [7-9], drug delivery [10-13], and wound repair [14-16], because of the high water content, biocompatibility and the thermoresponsive properties. The thermoresponsive hydrogels with 3-D networks formed by the physical crosslinks of thermoresponsive polymers can undergo reversible sol–gel transition as temperature changes. The polymers exhibiting lower critical solution temperature (LCST) are particularly attractive [17-19]. In this case, therapeutic agents, such as drugs, cell, or DNA can be simply blended with the aqueous polymer solutions at room temperature and injected into human body. The gelation can be triggered by the body temperature and achieve the controlled and local release of the therapeutic agents.

The design criteria of the thermoresponsive polymers are: i) the polymer and the decomposition product (if any) of the polymer should be biocompatible and noncytotoxic; ii) the thermoresponsive properties can be easily tailored, for example the near body temperature gelation temperature; iii) the polymer solution at room temperature should possess low viscosity, thus offering easy injectability; and iv) rapid gelation upon injection. Recently, the oligo ethylene glycol (OEG) methyl ether methacrylate monomers have gained great attention because they can meet all the above design criteria [9,20-26]. This family of monomer provides many choices with a change in the length of the OEG side chains, from hydrophobic ones, e.g., methoxy ethylene glycol methacrylate (MEGMA) to hydrophilic ones, e.g., methoxy oligo (ethylene glycol) methacrylate (OEGMA, M_n = 300 g mol^{-1}) [20,27-29]. The polymers based on these monomers shows good anti-fouling properties, no hysteresis, and are non-ionic therefore won't disturb the ion balance in body fluid [30,31]. Besides, the thermoresponsive properties of these polymers can be easily tuned by changing the molar mass (MM), structure, and composition [21,22,32-34]. These monomers can be synthesised via a living polymerisation method called group transfer

* Corresponding author at: Department of Materials, Royal School of Mines, Exhibiton Road, Imperial College London, SW7 2AXZ, London, UK.
E-mail address: t.georgiou@imperial.ac.uk (T.K. Georgiou).

https://doi.org/10.1016/j.eurpolymj.2023.112144
Received 20 March 2023; Received in revised form 7 May 2023; Accepted 8 May 2023
Available online 18 May 2023

polymerisation (GTP), which is less time consuming, cheaper, more efficient and easy to scale up than other living polymerisation methods [35-39].

In previous studies, people have extensively investigated the copolymers of di(ethylene glycol) methyl ether methacrylate (DEGMA) and OEGMA (300 g mol^{-1}) [18,30,40-43]. The cloud point (T_{CP}) of the OEGMA-DEGMA copolymer can be simply altered between 26 °C and 75 °C by adjusting the composition, because DEGMA shows a T_{CP} at around 26 °C and OEGMA exhibit a T_{cp} at 90 °C. Most of this research focused on the statistical polymer based on these two monomers. However, the statistical polymers lack the ability to form stable 3-D network and only present aggregation and precipitation at high temperature. Amphiphilic block polymers, however, are well known for their self-assembly ability in aqueous solutions [18,30,43-49]. These polymers can spontaneously self-assemble into a wide range of micelles with different morphologies, such as spheres, worms, vesicles, *etc* [50-55]. Some polymers can undergo the transition of one micelle morphology to another upon temperature changes. For example, Brotherton et al. [56], Raphael et al. [57], and Cunningham et al. [54], observed sphere-to-worm transition in diblock polymers. Ratcliffe *et al* observed sphere-worm-vesicle transition in poly(*N*-(2-hydroxypropyl) methacrylamide)-poly(2-hydroxypropyl methacrylate) (HPMAC-*b*-HPMA) diblock copolymer [58]. Several people reported the polymerisation-induced micelle transition [59-63]. Although OEGMA was extensively used as the thermoresponsive hydrophilic block in amphiphilic block polymers [41,43,64-68], very few studies investigated polymers where both the hydrophilic and hydrophobic monomers are based EG-based. In those studies, when linear polymers were investigated no gelation was observed. Interestingly, when star polymers based on OEGMA (475 g mol^{-1} – roughly 9 groups of EG) and DEGMA monomers were investigated and gelation was observed around body temperature [26,69-71]. However, these star polymers were found to show cytotoxicity at the gelation concentration in the cell viability tests and thus their biomedical application was limited.

Here, we report the synthesis of linear OEGMA-MEGMA copolymers via GTP. To the best of knowledge this the first time that diblock copolymers based on these monomers has been investigated. The molar mass (MM) was kept constant, targeted 8100 g mol^{-1} while the composition of the diblock copolymers was systematically varied. Specifically, in order to investigate how the composition affects the thermoresponsive properties of the polymers, the mass ratio of OEGMA to MEGMA was varied from 80 to 20, 70–30, 60–40, 50–50, 40–60, to 30–70. One statistical copolymer (50–50 wt%) was also synthesised for comparison (as schematically illustrated in Fig. 1). The thermoresponsive and self-assembled properties of the copolymers were studied in aqueous media with turbidimetry, dynamic light scattering (DLS), rheology and transmission electron microscopy (TEM), revealing some interesting temperature induced self-assembly restructuring. Finally, the thermoresponsive properties of the mixtures of the in house-synthesised copolymers with Pluronic® F127 were also studied.

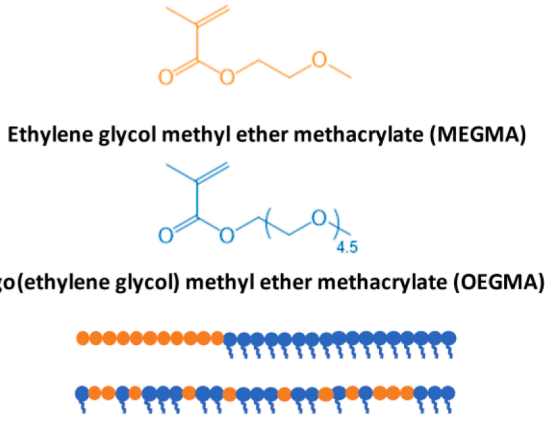

Fig. 1. Chemical structures, names, and abbreviations of the monomers and schematic illustration of the chemical structure of the copolymer synthesised in this paper.

2. Materials

The chemical structures of the two monomers used MEGMA, and OEGMA are shown in Fig. 1. MEGMA (MM = 144.17 g mol^{-1}, 99%) and OEGMA (average MM = 300 g mol^{-1}, contains 100 ppm MEHQ and 300 ppm BHT as inhibitor), methyl trimethylsilyl dimethyl ketene acetal (MTS, 95%), tetrahydrofuran (THF, anhydrous, HPLC grade, ≥99.9%), basic aluminium oxide (Al_2O_3·KOH), calcium hydride (CaH_2, ≥90%), 2,2-diphenyl-1-picrylhydrazyl hydrate (DPPH), thiazolyl blue tetrazolium bromide (HPLC, ≥97.5%), dimethyl sulfoxide (≥99.9%), branched polyethylenimine (PEI, 10000 g mol^{-1}), foetal calf serum (FCS, heat inactivated) and deuterated chloroform ($CDCl_3$, 99.8 atom % D) were purchased from Sigma Aldrich, United Kingdom·THF (GPC grade), phosphate buffered saline (PBS, solution), Dulbecco's Modified Eagle Medium/Nutrient Mixture F-12 (DMEM/F-12), and Penicillin-Streptomycin (10000 U/mL) were purchased from Fisher Scientific, United Kingdom. Ethanol, acetone, and *n*-hexane were purchased from VWR chemicals. AGS160 carbon film on 200 mesh grid copper were purchased from Agar Scientific Ltd, United Kingdom. ARPE-19 cells were obtained from Prof. Molly Stevens (Imperial College London, London, United Kingdom).

Tetrabutylammonium bibenzoate (TBABB) was in house synthesised, following the procedure reported by Dicker et al. [72].

3. Experimental

3.1. Synthesis of the polymers

All the polymers in this work were synthesised via GTP. The monomers, MEGMA and OEGMA, were purified by passing through the column with Al_2O_3·KOH twice to remove the inhibitor and acidic impurities. We used anhydrous THF as the solvent, MTS as the initiator and TBABB as the catalyst. MEGMA was freshly distilled at 45 °C on the day of synthesis. OEGMA was dissolved in anhydrous THF to prepare a 50% vol solution. The aimed structures are diblock and statistical. The mass ratio of MEGMA and OEGMA was varied from 80:20, 70:30, 60:40, to 50:50.

To synthesise the statistical polymer $OEGMA_{13}$-*co*-$MEGMA_{27}$, 10 mg of TBABB, 51.3 ml of THF, 9.9 ml of MEGMA and 18.8 ml of OEGMA solution was added to a 250 ml round bottom glass flask and stirred under argon. Then, 0.5 ml of MTS was added to the flask. An exotherm was detected and the reaction flask was then placed in water bath. The reaction was completed after 15 min. Samples were withdrawn for gel permeation chromatography (GPC) and nuclear magnetic resonance (NMR) analysis.

Sequential monomer addition was used to synthesise the diblock polymers. For example, for $OEGMA_{13}$-*b*-$MEGMA_{27}$, 10 mg of TBABB, 51.3 ml of THF and 0.5 ml of MTS were added to the flask and stirred under argon. 18.8 ml of OEGMA solution was then added dropwise to the reaction flask. An exotherm was observed. The mixture was allowed to react for 15 min to form the first block. Samples of the first block were withdrawn for GPC and NMR. Then 9.9 ml of MEGMA was added dropwise to the reaction flask and was allowed to react for another 15 min. GPC and NMR were withdrawn after 15 mins when the exotherm was depleted.

It should be noted that diblock polymers P1-4 were synthesised with OEGMA as the first block while diblock polymers P5 and P6 were synthesised with MEGMA as the first block. This is because when synthesised P5 and P6 with OEGMA first, the deactivation of the living polymer chain after the synthesis of the first block is not negligible. To address this problem, the sequence of the two blocks was altered.

All the successfully synthesised polymers were recovered by precipitation in *n*-hexane and were dried under vacuum over a week at room temperature.

3.2. Gel permeation chromatography (GPC)

An Agilent Security GPC system, with a polymer standard service (PSS), and a MIXED-D column (PL1110-6504, particle size [μm]: 5 μm, dimensions [mm]: 300 × 7.5 mm), an Agilent guard column (PL1110-1520, particle size [μm]:5, dimensions [mm]: 50 × 7.5, an Agilent 1250 refractive index (RI) detector and a "1260 Iso" isocratic pump was utilised to find out the molar mass (MM) and polydispersity index (*Đ*) of the precursors and the final products.

The GPC system was calibrated by poly(methyl methacrylate) (PMMA) standard samples with molar masses of 2000, 4000, 8000, 20000, 50000, and 100000 g mol^{-1}. The mobile phase was pure GPC grade THF. To prepare the GPC samples, the samples withdrawn from the reaction flask was diluted in 1 ml of THF and then filtered by a 0.45 μm PTFE syringe filter.

3.3. Proton nuclear magnetic resonance (^1H NMR) spectroscopy

A Jeol 400 MHz spectrometer instrument was used for NMR analysis. To prepare the NMR samples, the withdrawn samples from the reaction were dried under vacuum for 2 days and then redissolved in 650 μl of $CDCl_3$.

3.4. Ultraviolet–visible (UV–vis) spectroscopy

A Cary 3500 Compact Peltier UV–Vis System (Agilent) was used to determine the T_{cp} s of the 1% w/w solutions in DI water and PBS. The T_{cp} was determined as the temperature at which the transmittance of the 1% w/w solution dropped to 50%. The heating rate was controlled at 1 °C min^{-1} and the data point was collected every 1 °C at the wavelength of 550 nm. The samples were stirred at 600 rpm and held at each temperature point for 30 s.

3.5. Dynamic light scattering (DLS)

A Zetasizer Nano ZSP (Malvern) instrument was used to determine the hydrodynamic diameters of the polymers in 1% w/w DI water solutions. The samples were filtered through 0.45 μm nylon filter before the measurement. The measurement was conducted under room temperature (25 °C) and at a backscatter angle of 173°.

3.6. Transmission electron microscopy (TEM)

All the images were recorded under a JEOL STEM 2100Plus and a JEOL STEM 2100Plus transmission electron microscope. The transmission electron microscope was operated at 80 kV with a 70 μm objective aperture. The samples were 1 % w/w solutions in DI water and PBS. The grids were glow discharged by NanoClean model 1070, Fischione before use. Around 30 μl of the polymer solution was pipetted on to the glow discharged grids and then negatively stained by one drop of 2% w/v uranyl acetate for 60 s.

3.7. Visual test

An IKA RCT basic stirrer hotplate and an IKA ETS-D5 temperature controller was used for the visual test plot the phase diagram of the polymer. Different concentrations, 1, 2, 5, 10, 15, 20 and 25% w/w of the solutions in DI water and PBS solutions were investigated. The temperature range was 20 °C to 80 °C and the data was collected every 1 °C.

3.8. Rheology

A TA Discovery HR-1 hybrid rheometer with a geometry of 40 mm parallel plate was used to determine the rheological properties. A temperature ramp oscillatory test was conducted from 10 °C to 80 °C, with a heating rate of 1 °C min^{-1}, on the 15% w/w polymer solutions in DI water and PBS. The strain was 1% and the angular frequency was 1 rad s^{-1}.

3.9. Cell test

The cytotoxicity of the polymer was investigated in ARPE-19 cells by MTT assay. ARPE-19 cells were cultured at 37 °C and 5% CO_2 using DMEM/F12 medium. The culture medium was supplemented with 10% foetal calf serum, 100 U/mL penicillin, and 100 mg/mL streptomycin. Several concentrations of the polymer solutions (25, 50, 125, 250, and 500 μg mL^{-1}) were prepared. ARPE-19 cells were seeded on 96-well plates, at a density of 1 × 10ˆ(4)cells per well and then treated with the polymer solutions after 24 h. The cells were left to incubate for another 24 h. MTT solution (10%) was added to each well and left to incubate for 4 h. All wells were carefully aspirated, and crystals formed were solubilised with 100 μl of DMSO. Absorbance was read at 560 nm using a OPTImax microplate reader (Molecular Devices). Background absorbance was subtracted from readings to obtain final optical densities. PEI was used as positive comparison (cytotoxic control), the untreated cells represent the negative control to which the cell viability was established as 100%.

4. Result and discussion

In this work to investigate the thermoresponsive polymers based on the OEG-methacrylate monomers, one statistical and six diblock polymers based on MEGMA and OEGMA were synthesised. The target molar masses were 8100 g mol^{-1}. Based on our previous research on OEG-methacrylate monomers, the MEGMA was chosen as the hydrophobic block in the polymer, while the OEGMA was chosen as the thermoresponsive block. OEGMA is more hydrophilic at low temperature and is used to increase the solubility of the copolymer under room temperature.

4.1. Molar mass and composition

The molar masses and compositions of the polymers were confirmed by GPC and NMR and summarised in Table 1. The number average molar mass (M_n) of the diblock polymers (P1-6) are similar, in the range of 8000 to 9200 g mol^{-1}, slightly higher than the targeted M_n, as expected and observed before. Specifically, in previous GTP studies, the fact that the experimental MM was higher than the theoretical MM was attributed to some deactivation during the synthesis [40,52,73-76]. The deactivation is attributed to 1) the humidity introduced into the reaction flask during the additions; 2) the impurity in the OEGMA monomer. The OEGMA monomer was not distilled before synthesis due to the high MM and viscosity and was purified like in previous published studies [77]. Besides, it may also contain some hydroxy (non methacrylated) derivatives, which is well documented that affects the polymerisation [27,78]. The experimental MM of statistical polymer synthesised in this study was 12000 g mol^{-1}, higher than the theoretical value (8100 g mol^{-1}). The synthesis of the statistical polymer was repeated for 3 times and similar results were obtained in each batch. The discrepancy between the experimental MM of the diblock copolymers and the statistical copolymer was attributed to the water bath added to the reaction flask during the synthesis of the statistical copolymer in order to control the reaction's exotherm. Specifically, since the synthesis is a simultaneous addition, the initiator was added after all the monomers were added to the reaction flask. To avoid evaporation of the solvent due to violent exotherm during the reaction, a water bath was added to the reaction

Table 1
Theoretical chemical structures, Molar masses (theoretical and as experimentally determined by GPC) and molar mass distribution of the copolymers.

Sample No.	Theoretical chemical structure[a]	OEGMA content %		$MM^{c}_{theoretical}$ (g mol^{-1})	GPC result[b]	
		Theoretical	GPC[b]		M_n (±250 $gmol^{-1}$)	$Đ$
P1	$OEGMA_{21}$	80	77	6400	6500	1.18
	$OEGMA_{21}$-*b*-$MEGMA_{11}$			8100	8400	1.17
P2	$OEGMA_{19}$	70	73	5600	6700	1.14
	$OEGMA_{19}$-*b*-$MEGMA_{17}$			8100	9200	1.20
P3	$OEGMA_{16}$	60	63	4800	5800	1.14
	$OEGMA_{16}$-*b*-$MEGMA_{22}$			8100	9200	1.17
P4	$OEGMA_{13}$	50	55	4000	5000	1.12
	$OEGMA_{13}$-*b*-$MEGMA_{27}$			8100	9100	1.22
P5	$MEGMA_{33}$	40	33	4800	5300	1.11
	$MEGMA_{33}$-*b*-$OEGMA_{11}$			8100	8000	1.15
P6	$MEGMA_{38}$	30	28	5600	6300	1.09
	$MEGMA_{38}$-*b*-$OEGMA_{8}$			8100	8900	1.12
P7	$OEGMA_{13}$-*co*-$MEGMA_{27}$	50	50	8100	12,000	1.17

[a] MEGMA: ethylene glycol methyl ether methacrylate, OEGMA: oligo(ethylene glycol) methyl ether methacrylate.
[b] As determined by GPC using poly(methyl methacrylate) PMMA standard samples. The compositions of each copolymer were calculated based on the GPC result and not from the NMR because the characteristic peaks of the methyl group on the end of OEGMA and MEGMA merged with each other.
[c] The theoretical molar mass was calculated as $MM_{theoretical} = MM_{monomer} \times DP + 100\ g\ mol^{-1}$, here the $MM_{monomer}$ was the molar mass of the monomer; the DP was the degree of polymerisation of the corresponding block; the 100 g mol^{-1} was the MM of the fragment of the MTS initiator remaining on the polymer backbone.

flask before the polymerisation, and thus the statistical polymer was synthesised in a more humid environment. As GTP is an anionic polymerisation method, it is very sensitive to labile protons. Despite the higher MM, the $Đ$ value is 1.17 lower than 1.25 which still indicates that a well-defined statistical copolymer was obtained and thus was further characterised in terms of its aqueous properties [79,80]. In fact, the MM dispersity was satisfactory for all synthesised copolymers since the $Đ$ values ranged from 1.12 to 1.22 showing a narrow MM distribution for all copolymers.

As shown in Fig. 2, the GPC traces polymer P1, 4 and 7 are plotted. As shown in Fig. 2(a) and (b) the peaks shift to higher molar mass indicating the successful sequential addition of the second monomer. The absence of the monomer peak confirms the full conversion of the monomers and the successful synthesis of the polymers. The GPC curves of other copolymers can be found in the supplementary information, Fig. S1.

Since the characteristic peak of the methyl group on the end of OEGMA and MEGMA merged with each other, the compositions of each copolymer were calculated based on the GPC result and not from the NMR as it is the normal practice. The NMR spectra can be found in Fig. S2.

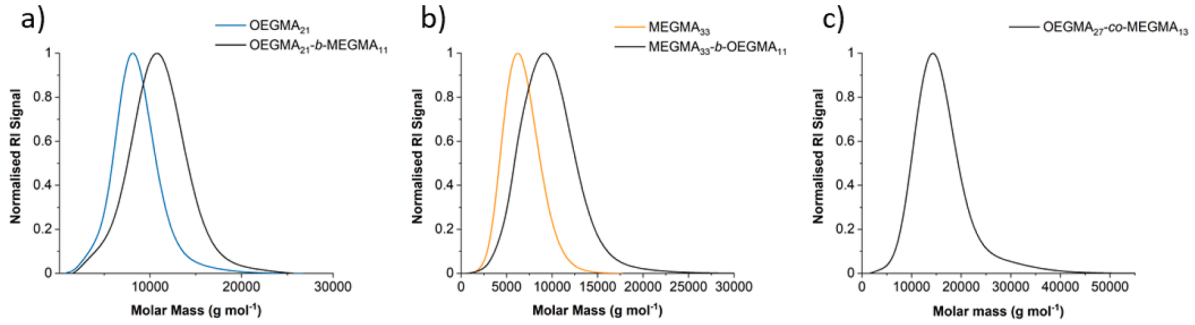

Fig. 2. GPC chromatogram of: a) P1 ($OEGMA_{21}$-*b*-$MEGMA_{11}$), the precursor ($OEGMA_{21}$) is plotted in blue and the final diblock copolymer is plotted in black; b) P5 ($MEGMA_{33}$-*b*-$MEGMA_{11}$), the precursor ($MEGMA_{33}$) is plotted in orange and the final diblock copolymer is plotted in black; c) P7 ($OEGMA_{21}$-*co*-$MEGMA_{11}$), the final product is plotted in black. (For interpretation of the references to colour in this figure legend, the reader is referred to the web version of this article.)

Table 2
Cloud points of 1% w/w polymer solutions in DI water and PBS determined by UV–vis.

Sample No.	OEGMA Content %	Theoretical chemical structure	Molar Mass (g mol^{-1})	Cloud point[a] (±1 °C)	
				DI	PBS
P1	77	$OEGMA_{21}$-*b*-$MEGMA_{11}$	8400	59	55
P2	73	$OEGMA_{19}$-*b*-$MEGMA_{17}$	9200	59	54
P3	63	$OEGMA_{16}$-*b*-$MEGMA_{22}$	9200	55	50
P4	55	$OEGMA_{13}$-*b*-$MEGMA_{27}$	9100	50	45
P5	33	$MEGMA_{33}$-*b*-$OEGMA_{11}$	8100	52	49
P6	29	$MEGMA_{38}$-*b*-$OEGMA_{8}$	8900	51	48
P7	50	$OEGMA_{27}$-*co*-$MEGMA_{13}$	12,000	28	23

4.2. Thermoresponsive properties

4.2.1. Cloud point

The T_{CP}) of 1% w/w polymer solution in DI water and PBS was determined by the UV–vis (Table 2). The UV–vis profiles can be found in Fig. S3. As shown in Table 2, the T_{CP}s of the diblock polymers in DI water were in the range of 50–59 °C, while the T_{CP} of the statistical polymer (P7) was 29 °C. The solution of the statistical polymer was slightly cloudy under room temperature (25 °C), indicating the presence of large aggregations in the solution.

Several parameters affect the T_{CP}, like the MM, the chemical structure but also the polymer architecture [81]. For example, block polymers can form micelles to stabilise themselves in solution, while the statistical polymers tend to form large aggregations and precipitate easier (at lower temperatures) from the solution when the temperature is elevated. This was observed in previous studies and also in the present study [23,47,49,82].

In terms of the chemical composition it has been previously reported, for polymers with similar chemistry, that the higher the hydrophobic/hydrophilic ratio, the lower the T_{CP} [27,52,85,91,104]. Furthermore in one study on statistical copolymers of the same chemistry the T_{CP} decreases as the OEGMA content decreased [40]. However in the present study where diblock copolymers are investigated, the T_{CP} does not linearly decrease as the OEGMA content decreases in the DEGMA-*b*-OEGMA diblock polymers. Specifically, a decrease was observed from P1 to P3 when the OEGMA content decreases from 77 to 63 wt% however this trend does not continue when the OEGMA content is lowered further. We believe that this is due to the different shape/morphology of the micelles/aggregates that are being formed as the hydrophobic/hydrophilic ration changes. This will be further discussed in the section of micelle morphology below. When comparing the TEM images taken under room temperature and T_{CP}, it was found that polymer P5 and P6 underwent micelle morphology transition from spherical micelles to worm-like micelles through micelle reassembly. This micelle reassembly was not observed in polymers with higher OEGMA content (P1-4). The micelle reassembly of P5 and P4 postpone the formation of the large aggregates and therefore retarded the precipitation.

When comparing the T_{CP}s in PBS to DI waster, the T_{CP}s in PBS were a few degrees lower than the ones in DI water, in line with the previous studies [45,69,88,89]. The OEG moiety is sensitive to the hydrated ions in PBS, thus the solubility of the copolymer was reduced. Due to the presence of the salts in the solution, the polymer chains are preferentially "salted out" from the solution and thus favour the precipitation [74,90].

Table 3
Theoretical hydrodynamic diameters calculated based on random coil assumption and micelle assumption and the experimental hydrodynamic diameters measured by DLS at 25 °C.

Sample No.	OEGMA Content %	Theoretical chemical structure	D_h (±0.5 nm)	Theoretical[a] (nm)
P1	77	$OEGMA_{21}$-*b*-$MEGMA_{11}$	6.8	17.8
P2	73	$OEGMA_{19}$-*b*-$MEGMA_{17}$	15.7	19.2
P3	63	$OEGMA_{16}$-*b*-$MEGMA_{22}$	15.7	19.2
P4	55	$OEGMA_{13}$-*b*-$MEGMA_{27}$	19.6	19.1
P5	33	$MEGMA_{33}$-*b*-$OEGMA_{11}$	50.7	18.9
P6	29	$MEGMA_{38}$-*b*-$OEGMA_{8}$	32.7	17.3
P7	50	$OEGMA_{27}$-*co*-$MEGMA_{13}$	348	3.3[b]

[a] The theoretical diameter was calculated by assuming the diblock copolymer formed spherical micelles in the solution based on the equation: $d = (13.5 + DP_1 + 2 \times DP_2) \times 0.252$ nm; here DP_1 and DP_2 is the degree of polymerisation of the first and second block, calculated based on the result of GPC, 13.5 is the converted DP of the ethylene glycol (EG) groups on the side chain.

[b] The theoretical diameter was calculated by assuming the statistical polymer formed random coil in the solution based on the equation: $(d_g)^{1/2} = 2 \times (2 \times 2.20 \times (6.75 + DP_{total})/3)1/2 \times 0.154$ nm; here DP_{total} is the total degree of polymerisation of both monomers, calculated based on the result of GPC.

4.2.2. Micelle morphology

The self-assembly of the diblock copolymers in water was examined by DLS and TEM. As shown in Table 3, the hydrodynamic diameters determined by DLS are compared with the theoretical calculations. The DLS histograms can be found in Fig. S4 in the supplementary information. The theoretical calculation was based on spherical micelles for the diblock polymer and on the random coil for the statistical polymer, as reported in our previous work [40,91]. For the diblock polymers, it is assumed that the MEGMA blocks overlapped to form the hydrophobic core and the OEGMA block formed the hydrophilic corona of the spherical micelles. Due to the lengthy side chain on OEGMA, the length of the side chain should be taken into consideration when calculating the diameter of the spherical micelle. The length of the EG group is considered as 1.5 times of the methacrylate and there are 4.5 EG groups on the side chain. Therefore, the converted DP of the OEG side chain is 6.75 (1.5 × 4.5). There are two OEGMA end group in the corona, thus the 13.5 (2 × 6.75) was added to the DP when doing the calculation.

The hydrodynamic diameter of P2-4 is very close to the theoretical calculation, confirming the self-assembly into spherical micelles of these polymers. The experimental result is slightly smaller than the calculated result, as expected, because the calculation is based on the assumption that all the polymer chains are fully stretched. P1 ($OEGMA_{21}$-*b*-$MEGMA_{11}$), the diblock polymer with the highest OEGMA content (77% w/w), was found to exist as unimers rather than spherical micelles under room temperature. This is attributed to: 1) the overall high hydrophilicity of P1 due to the high OEGMA content; 2) the short MEGMA block which is not long enough to form a stable hydrophobic core. Since the micelle formation is a hydrodynamic process achieved by the assembly and the disassembly of the polymer chain, the stability of the micelle is dependent on the hydrophobic core. Therefore, the polymer chains of P1 exists in the solution mainly as unimers rather than micelles because the MEGMA block of P1 is too short to maintain a stable micelle structure.

P5 and P6, the diblock polymers with higher MEGMA content (67% w/w and 72% w/w), were found to form micelle clusters and bigger aggregates in DI water under room temperature. This observation is in agreement with the visual observation of the slightly cloudy solutions under room temperature and the clusters observed in the TEM images, as shown in Fig. 3.

The micelle morphology of P4,5 and 6, at both room temperature and T_{CP} was investigated under TEM. TEM images taken at room temperature in both PBS and DI water and the TEM images taken at T_{CP} in DI water are presented in Fig. 3. The polymer solutions were heated to the T_{cp}, and immediately dropped onto the TEM grids to secure the micelle morphology at that temperature. As shown in Fig. 3 (1st row), at room temperature, spherical micelles are observed for all three copolymers. In the TEM images of P5 and P6, micelles with different sizes and micelle clusters are observed, while in the TEM image of P4, micelles with similar sizes are observed. The average micelle diameters measured in the TEM images for P4-6 are 24.8 nm, 24.9, and 25.6 nm, respectively, which are in line with the hydrodynamic diameters obtained from DLS.

Interestingly, at T_{CP}, larger spherical micelles and micelle clusters are observed for P4, while worm-like micelles are observed for P5 and P6, as shown in Fig. 3 (3^{RD} row). P5 and P6 undergo temperature triggered micelle morphology transition from spherical micelle to "worm-like" micelle at T_{CP}. The co-existence of spherical micelles and "worm-like" micelles is observed in the TEM image of P5 taken at T_{CP}. It is found that the average micelle size of the spherical micelle of P5 grows from 24.9 nm to 49.2 nm. The diameter of the cross section of the "worm-like" micelles of P5 and P6 is 40.2 nm and 21.4 nm, respectively, which is similar to the diameter of the spherical micelle. Therefore, we assume the micelle morphology transition is achieved by the secondary assembly of the spherical micelles. This is supported by the observation of intermicellar branching junction in the TEM images of P5 and P6 taken at T_{CP}. The temperature triggered micellar growth and micellar transition was widely reported on PEG-derived surfactant, such as polyoxyethylene cholesteryl ether [92,93], polyoxyethylene alkyl ether [94,95],

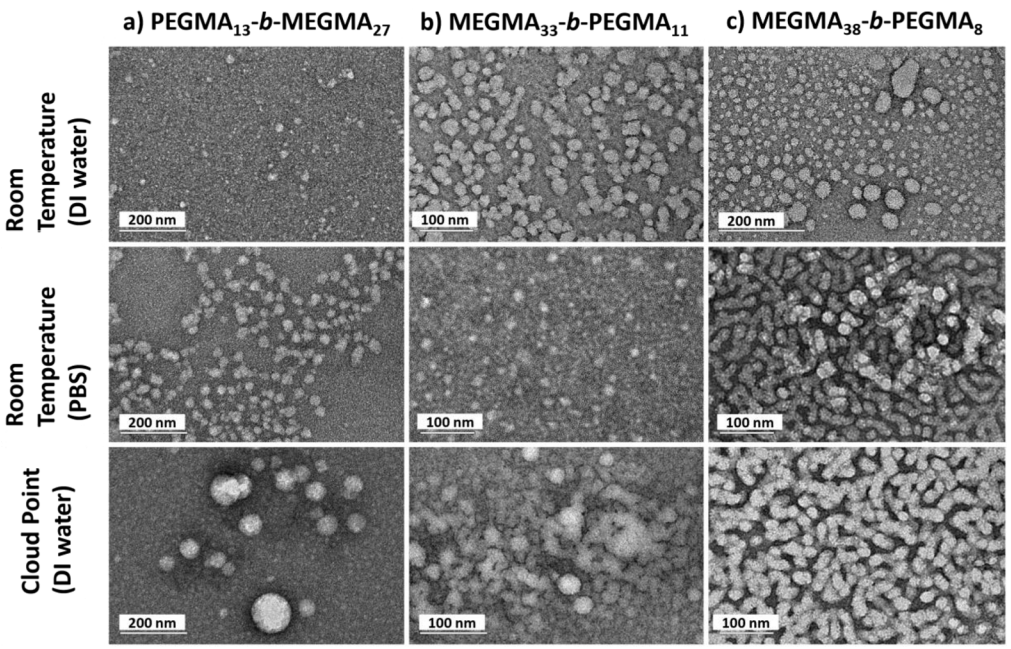

Fig. 3. TEM images of P4 ($OEGMA_{13}$-b-$MEGMA_{27}$), P5 ($MEGMA_{33}$-b-$OEGMA_{11}$) and P6 ($MEGMA_{38}$-b-$OEGMA_{8}$) in 1 % w/w DI water at room temperature (1st row), in 1 % w/w PBS at room temperature (2nd row) and, in 1 % w/w DI water at cloud point (3rd row).

etc. The driven force of the micellar growth and the micellar transition of the PEG-derived surfactant is the dehydration of the PEG headgroup upon heating. During the heating process, the interfacial curvature of the spherical micelle or aggregate decreases due to the dehydration of the PEG headgroup, which leads to the micellar growth. Upon heating, due to the further dehydration of the PEG headgroup and the decrease in the interfacial curvature, spherical micelles start to merge to form rod-like micelles. These rod-like micelles are connected by the inter-micellar branching junctions to form infinitely long worm-like micelles. Similar explanation can be applied to the micelle morphology transition observed for P5 and P6.

Gao *et al* reported polymerisation induced spherical to worm-like micelle transition on diblock polymer OEGMA-*b*-DAAM diacetone acrylamide (DAAM) and found that the micelle morphology is related to the DP of the hydrophobic group [59]. They found only diblock copolymers with sufficient length of DAAM block can form "worm-like' micelles or vesicles while diblock polymers with short DAAM block only form spherical micelles. Besides, it was found that if switching the hydrophilic block $OEGMA_{15}$ with a more hydrophilic block $OEGMA_{38}$, the sphere-sphere fusion was prevented. The micellar transition is governed by the overall hydrophobic/ hydrophilic balance of the polymer. Our diblock polymers exhibit similar behaviour, i.e., P4 with short MEGMA block only form spherical micelles while P5 and P6 form worm-like micelles at T_{CP}. The micelle morphology is the result of the equilibrium of the interactions between the polymer chains and water [96]. To avoid the interaction between the hydrophobic block and the water molecules, because this interaction is less energetically favourable, micelle structures with different interfacial curvatures are formed. The hydrophobic/ hydrophilic ratio between the two blocks controls the interfacial curvature and thus diblock copolymers with different hydrophobic content self-assemble into different morphologies at. As a result of the hydrophobic/ hydrophilic balance between the two blocks, P4 undergo size growth while P5 and P6 undergo spherical to worm-like micelle transition at elevated temperature.

Due to the formation of the "worm-like" micelles, the thermal responsive behaviour of P5 and P6 is different from P4. As discussed in the previous section, the T_{CP} of P4 which has higher OEGMA content, is lower than the T_{CP} of P5 and P6. We believe that the secondary assembly of the micelles formed by P5 and P6 at the T_{cp} prevents the formation of large aggregations at this temperature and therefore postpone the precipitation (phase separation). The temperature triggered micelle morphology transition of P5 and P6 also leads to the difference in the hydrogel structure, which will be further discussed in the next section.

4.3. Phase diagram of copolymers

The phase diagrams of the copolymer solutions were plotted based on the visual observations of the polymer solutions in DI water and PBS with various concentrations (1, 2, 5, 10, 15, 20, 25 % w/w). As shown in Fig. 4, the solutions in DI water of the most hydrophobic diblock polymers, specifically, of P4, P5 and P6 with an OEGMA content of 55% w/w, 33% w/w and 29% w/w form gels. The phase diagrams of the other copolymers and the phase diagrams in PBS, can be found in Figs. S5-9, which only show precipitation of the polymer as the temperature increases. In terms of the phases diagrams of P4-P6 in PBS similar observations are made to the phase diagrams in DI water that are shown in Fig. 4. The main difference is that the T_{gel} in PBS was observed a few degrees lower than that observed in DI water due to the "salting out" effect [69].

Interestingly, P4 with the highest OEGMA content (55 % w/w) forms gel at lower concentration (5% w/w) than the other two copolymers (10 and 15 % w/w). However, the gelation temperature window of the P4 is narrower than the other two copolymers. This is explained by the difference of the micelle morphology between P4 and the other two polymers. Although they all form core–shell micelles under room temperature, due to the difference in the length of the OEGMA block, P4 forms "star-like" micelles and P5 and P6 forms "crew-cut" micelles as shown in Fig. 5. We believe that the formation of physical entanglement between micelles is more likely to occur in "star-like" micelles that have a longer corona, compared to "crew-cut" micelles with a shorter corona (micelles with short hydrophilic chains around the corona). Besides, as discussed in the micelle morphology section, the micelle formed by P4 is less stable because MEGMA block of P4 is relatively short. It is hypothesised that the gelation happens when these unstable smaller micelles start bridging and this is undertaken at lower temperatures compared to the gelation temperatures of P5 and P6. On the other hand, the higher gelation temperatures, and broader gelation temperature windows of P5 and P6 are attributed to the micelle morphology

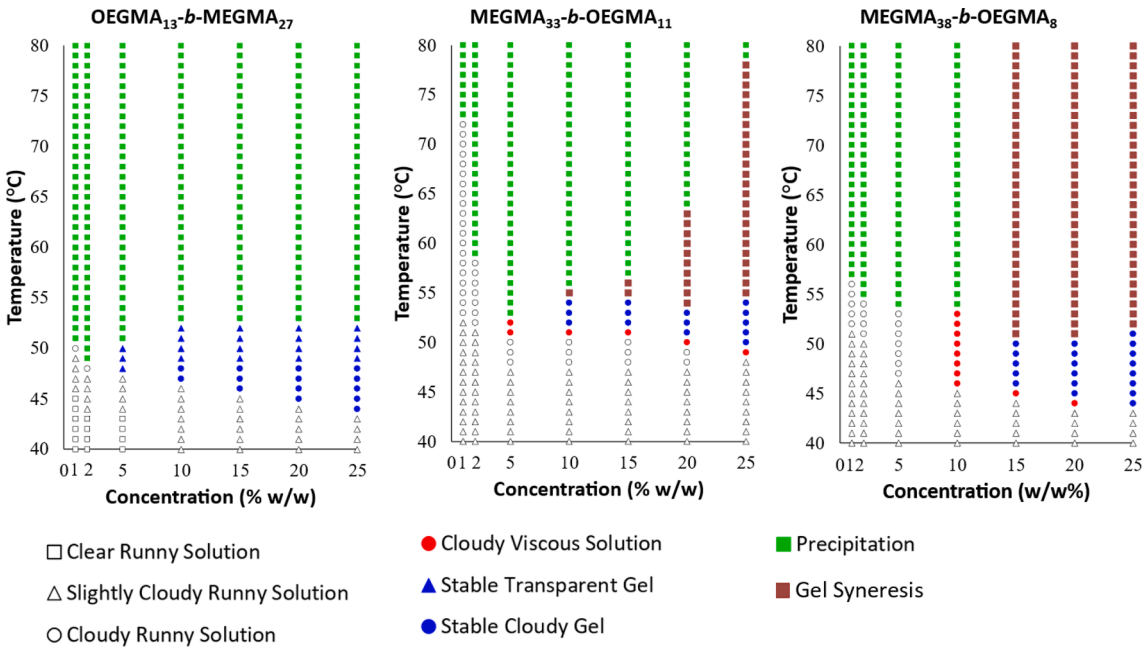

Fig. 4. From left to right, the phase diagrams of P4 ($OEGMA_{13}$-b-$MEGMA_{27}$), P5 ($MEGMA_{33}$-b-$OEGMA_{11}$) and P6 ($MEGMA_{38}$-b-$OEGMA_8$) in DI water. The concentration of the solution was varied from 1% w/w to 25% w/w. The transparent solution, slightly cloudy solution, cloudy solution, cloudy viscous solution, stable cloudy gel, stable transparent gel, gel syneresis and precipitation was indicated by square, triangle, circle, red circle, blue circle, blue triangle, brown square, and green square, respectively. (For interpretation of the references to colour in this figure legend, the reader is referred to the web version of this article.)

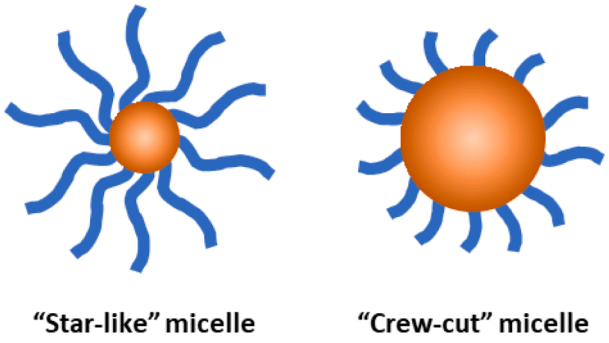

Fig. 5. Schematic illustration of star-like micelle and crew cut micelle.

transition. As discussed, P5 and P6 undergo temperature triggered transition from spherical micelle to "worm-like" micelle through while P4 only forms spherical micelles. Therefore, there is a difference in the gel structure between P4 and the other two copolymers. The hydrogel formed by P4 is through the close packing of the spherical micelles [33,97] while the hydrogel formed by P5 and P6 is through the entanglement of "worm-like" micelles [33,54,62,63]. Since the micellar lattice of the hydrogel formed by P4 is connected by the interactions between the PEGMA corona, the micellar lattice can be disrupted by the collapse of the PEGMA corona due to the "hydrophobic effect" at elevated temperature. While the hydrogel formed by P5 and P6 is connected by the intermicellar branching junctions and the physical entanglement between the worm-like micelles and thus the 3-D network stays stable until both connections are disrupted by the dehydration of the OEGMA block. Therefore, the gelation temperature window of P4 is relatively narrower than the other two copolymers.

No temperature triggered gelation was observed for the statistical polymer because the statistical polymer was not able to self-assemble to form micelles. As temperature increases, the polymer chains coil and form large aggregates to decrease the interaction with water molecules due to the increase of the hydrophobicity of the OEGMA. Therefore, the statistical polymer tends to precipitate from the solution rather than for hydrogel network as temperature is elevated. Diblock polymers with OEGMA content higher than 55% w/w (P1-3) failed to undergo sol–gel transition due to the insufficient length of the hydrophobic block. The thermal gelling behaviour of the diblock polymer is highly dependent on the hydrophobic / hydrophilic balance of the hydrophobic block (MEGMA block) and the thermoresponsive block (OEGMA block). As observed in the DLS result, P1 exists in water solutions as unimers rather than micelles due to the high OEGMA content. Therefore, P1 behaves similar to the statistical polymer. Although micelle formation is observed for P2 and P3, the micelle structure is less stable when compared with the copolymers with longer MEGMA block. Due to the insufficient length of the MEGMA block of P2 and P3, the hydrophobic core is loosely packed due to the lack of entanglement between the MEGMA blocks and thus micelles with a less compacted structure are formed. Therefore, at elevated temperature, the micelles of P1-3 readily collapse and precipitate from the solution rather than forming a 3-D connected network through close packing.

4.4. *Phase diagram of the mixture with Pluronic® F127*

The mixtures of the copolymers P4-7 with Pluronic® F127 was also investigated visually. The total concentration of the mixture was kept the same at 25% w/w. The concentration of Pluronic® F127 was varied from 5% w/w, 10% w/w, 12.5% w/w, 15% w/w to 20% w/w. As shown in Fig. 6, the phase diagrams of the mixtures were compared.

We found that all the copolymers broadened the gelation area of Pluronic® F127 by lowering the gelation concentration and increasing the upper boundary of the gelation region. The diblock polymers, P4 and P5 lowered the gelation concentration of Pluronic® F127 to 5% w/w. The gel formed at 5% w/w of Pluronic® F127 stayed stable until up to 80 °C. On the other hand, $OEGMA_{38}$-*b*-$MEGMA_8$ only lowered the gelation concentration to 12.5% w/w. In our previous study, the statistical polymer OEGMA-*co*-BuMA-*co*-DEGMA was not soluble when mixed with Pluronic® F127. Interestingly, in this study the statistical copolymer P7, although it doesn't form gel on its own, seems to assist the gelation of Pluronic F127, by lowering the critical gelation

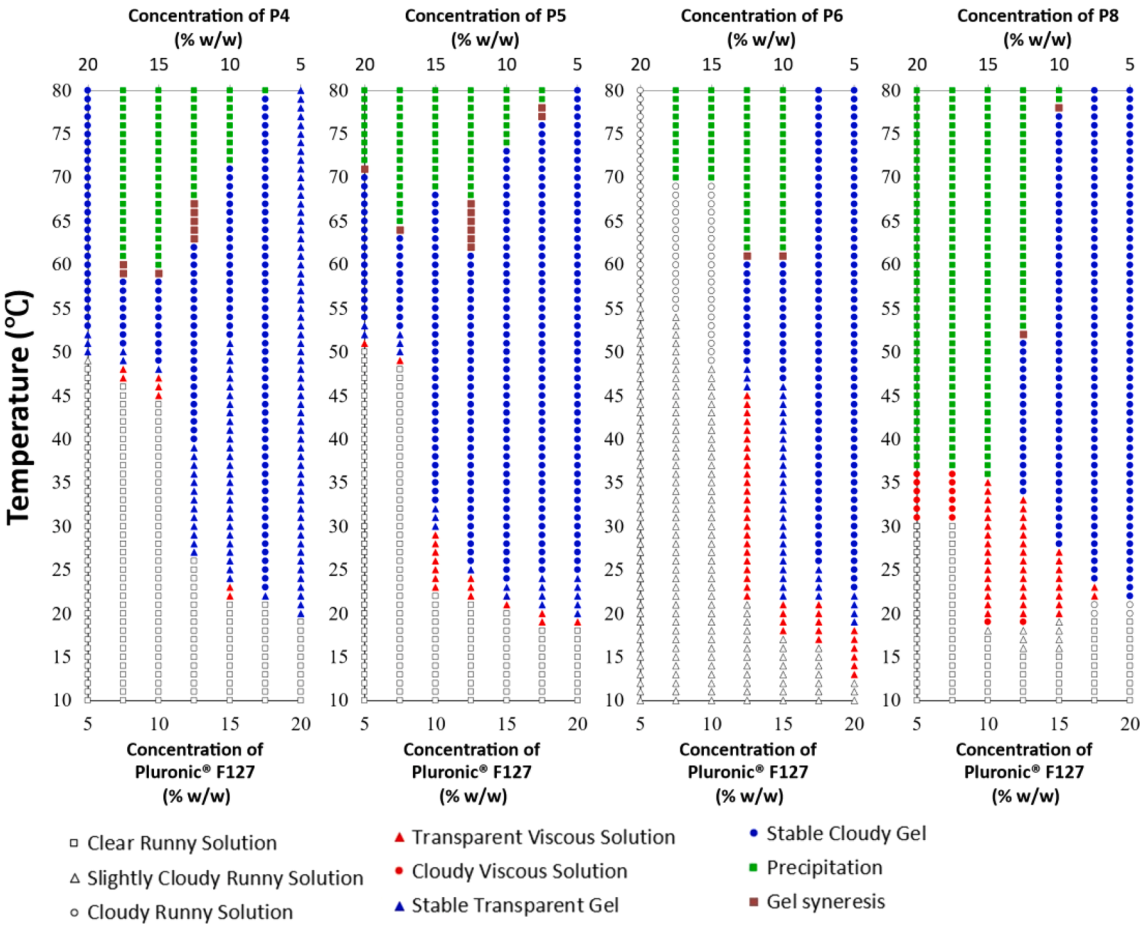

Fig. 6. The phase diagrams in DI water for the binary mixtures of Pluronic® F127 with copolymer, from left to right, P4 ($OEGMA_{13}$-b-$MEGMA_{27}$), P5 ($MEGMA_{33}$-b-$OEGMA_{11}$), P6 ($MEGMA_{38}$-b-$OEGMA_{8}$) and P7 ($OEGMA_{27}$-*co*-$MEGMA_{13}$). The total concentration of the solution was kept at 25% w/w; the concentration of Pluronic F127 was varied from 5% w/w to 20% w/w. The transparent solution, slightly cloudy solution, cloudy solution, cloudy viscous solution, stable cloudy gel, stable transparent gel, gel syneresis and precipitation was indicated by square, triangle, circle, red circle, blue circle, blue triangle, and green square, respectively. (For interpretation of the references to colour in this figure legend, the reader is referred to the web version of this article.)

concentration of Pluronic® F127 from 15% w/w to 12.5% w/w with a gelation window from 34 °C to 48 °C. It was found that by mixing the Pluronic® F127 with reverse poloxamer (PPO-PEO-PPO), the gelation temperature could be lowered by decreasing the "effective" concentration of Pluronic® F127 [98-100]. The PEO group in the reverse poloxamer can associate with the water molecules and decrease the water content around Pluronic® F127. The Pluronic® F127 is more "concentrated" with the presence of the reverse poloxamer and thus sol–gel transition happens at lower temperature. The effect of reverse poloxamer with higher PEO content on the gelation behaviour of Pluronic® 127 is more profound due to the more significant water association. Similarly, diblock copolymers with higher OEGMA content (P4 and P5) can lower the gelation concentration further than the diblock polymer with lower OEGMA content (P6). It appears that these diblock polymers can bridge the micellar lattice formed by Pluronic® 127.

4.5. Rheology

Oscillatory temperature ramp test was conducted to investigate the gelation behaviour of the 15% w/w polymer solutions of P4, P5, and P6 in PBS and DI water. As shown in Fig. 7, the loss modulus (viscous modulus) and storage (elastic modulus) modulus was plotted against the temperature. The rheological curve of DI water solutions can be found in Fig. S10 in the supplementary information. The rheological T_{gel} and visual T_{gel} are compared in Table 4.

As observed in the rheological curve, at low temperatures, the polymer exists in the solution as micelles and thus the viscosity of the solution is low. Upon heating, an elastic 3-D network is formed in the mixture, thus the elastic modulus becomes larger than the viscous modulus. The crossover point of the viscous modulus and the storage modulus is defined as the gelation point [101]. The gelation points given by the rheology tests are in good agreement with the visual tests within the error of the technique (±1 °C) as shown in Table 4. A second crossover of the two moduli was observed a few degrees after the gelation point, due to the shrinkage and collapse of the 3-D network. This was confirmed by the gel syneresis followed by precipitation at higher temperature observed during the visual test. The mechanical strength of the hydrogel formed by P5 and P6 is slightly lower than P4. This is due to the difference between the gel structure of P4 and P5, 6. As discussed previously, the gel structure of P4 is an ordered lattice formed by the close packing of the core–shell micelles while the gel structure of P5,6 is a 3-D network connected by the intermicellar branching junctions and the entanglements of the "worm-like" micelles. Since the intermicellar junctions can slide over the "worm-like" micelles and thus the hydrogel formed by P5 and P6 is softer than P4.

4.6. Cytotoxicity

The cytotoxicity of three diblock copolymers with thermal responsive gelation behaviour identified in this study was investigated in ARPE-19 cells by MTT assay. MTT assay was used to evaluate the effects of polymer on metabolic activity of the cells because of its high

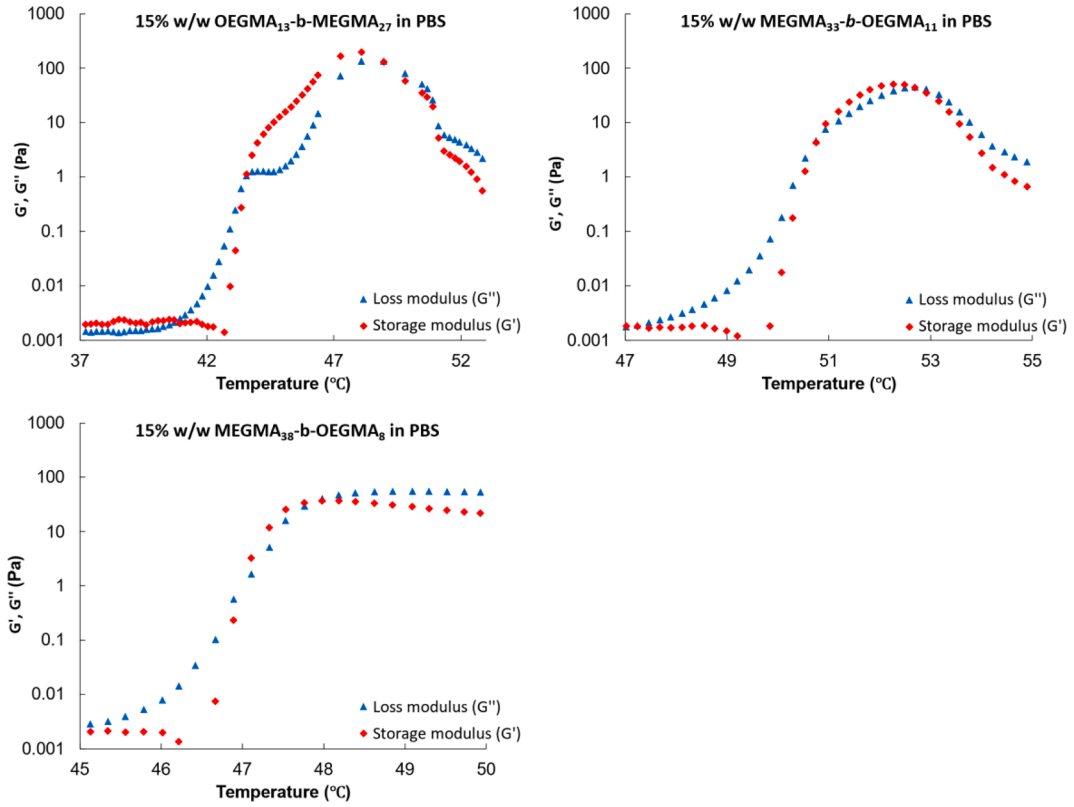

Fig. 7. Loss modulus (blue triangle) and storage modulus (red diamond) as a function of temperature of the copolymer solutions in PBS at 15% w/w. (For interpretation of the references to colour in this figure legend, the reader is referred to the web version of this article.)

Table 4
The gelation temperature of 15% w/w copolymer in DI water solutions determined by visual test and rheometer.

Sample	Theoretical Chemical structure	T_{gel} (°C)	
		Visual (±2)	Rheometer (±1)[a]
P4	$OEGMA_{13}$-*b*-$MEGMA_{27}$	46	47
P5	$MEGMA_{33}$-*b*-$OEGMA_{11}$	52	51
P6	$MEGMA_{38}$-*b*-$OEGMA_8$	46	47

[a] The gelation point is determined as the temperature at the first crossover of storage modulus and loss modulus.

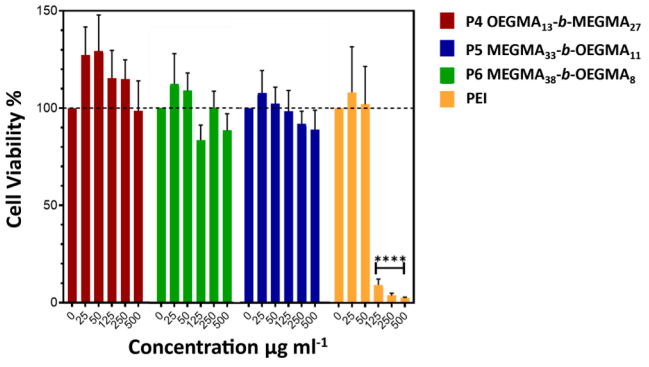

Fig. 8. Relative ARPE-19 cell viability as a function of polymer concentration. The P4 ($OEGMA_{17}$-b-$MEGMA_{28}$), P5 ($MEGMA_{33}$-b-$OEGMA_{11}$), P6 ($MEGMA_{38}$-b-$OEGMA_8$) and PEI is coloured in red, blue, green, and orange, respectively. (For interpretation of the references to colour in this figure legend, the reader is referred to the web version of this article.)

sensitivity, reliability of quantitation and ease of use. PEI, known for the toxicity was used as a positive (cytotoxicity) control [102]. As shown in Fig. 8, the cell viability was plotted against the concentration of the polymer solution. The cell viability of the polymer was calculated relative to the cell viability of the untreated cell, which was kept at 100%.

There were no significant differences in cell viability in the presence of these polymers with the untreated cells. Therefore, the polymers tested showed good cell viability with ARPE-19 cells for the time (48 h) and concentrations (25, 50, 125, 250, and 500 µg mL^{-1}) tested. As expected, the PEI control group was proved toxic to the ARPE-19 cells with a loss in cell viability up to 90% at the 3 highest concentrations. It seems that P4 showed higher cell compatibility than the other copolymers. As reported in a review by the O'Reilly's group [103], the correct overall hydrophilic/ hydrophobic balance of the copolymer is crucial to the cell viability. It was found that copolymer with insufficient hydrophobic content could prevent the protein attachment and cell adhesion, while copolymers with too high hydrophobic content could result in denaturation and difficulties in protein release. Therefore, P4 was found to have the most beneficial hydrophilic/ hydrophobic balance for cell viability among all three diblock copolymers.

5. Conclusion

In conclusion, we successfully synthesised statistical and diblock thermoresponsive copolymers based on OEGMA and MEGMA with good cell compatibility. All copolymers were investigated in terms of their thermoresponsive properties. The T_{cp} of the OEGMA-*b*-MEGMA diblock polymer doesn't have a linear relationship with the OEGMA content as reported in the statistical polymer. This was due to the transition of the spherical micelles to the worm-like micelles which happened in diblock polymers with higher MEGMA content as temperature increased. The TEM pictures recorded at T_{cp} confirms the micelle morphology

transition. It's assumed that the micelle morphology transition is through the secondary assembly of the spherical micelles. Interestingly, the diblock copolymers with the lowest OEGMA content formed gels and to the best of our knowledge is the first time that PEG-based linear copolymers are reported to form gels. In addition, the mixtures of the copolymers and Pluronic® F127 were also investigated. The copolymers broaden the gelation window of Pluronic® F127, among which, the statistical polymer lowered the gelation concentration of Pluronic® F127 to 12.5% w/w with a T_{gel} at 34 °C. This formulation mixture shows promise for applications like drug delivery and in tissue engineering as an injectable gel.

Declaration of Competing Interest

The authors declare that they have no known competing financial interests or personal relationships that could have appeared to influence the work reported in this paper.

Data availability

Data will be made available on request.

Appendix A. Supplementary material

Supplementary data to this article can be found online at https://doi.org/10.1016/j.eurpolymj.2023.112144.

References

[1] S. Bahl, H. Nagar, I. Singh, S. Sehgal, Smart materials types, properties and applications: a review, Mater. Today Proc. 28 (2020) 1302–1306.
[2] S.J. Buwalda, et al., Hydrogels in a historical perspective: from simple networks to smart materials, J. Control. Release 190 (2014) 254–273.
[3] M. Sponchioni, U. Capasso Palmiero, D. Moscatelli, Thermo-responsive polymers: applications of smart materials in drug delivery and tissue engineering, Mater. Sci. Eng. C 102 (2019) 589–605.
[4] K.J. Hogan, A.G. Mikos, Biodegradable thermoresponsive polymers: applications in drug delivery and tissue engineering, Polymer (Guildf) 211 (2020), 123063.
[5] M.T. Cidade, et al., Injectable hydrogels based on pluronic/water systems filled with alginate microparticles for biomedical applications, Materials (Basel) 12 (2019).
[6] M.T. Cook, P. Haddow, S.B. Kirton, W.J. McAuley, Polymers exhibiting lower critical solution temperatures as a route to thermoreversible gelators for healthcare, Adv. Funct. Mater. 31 (2021).
[7] Y. Zhang, et al., Thermosensitive hydrogels as scaffolds for cartilage tissue engineering, Biomacromolecules 20 (2019) 1478–1492.
[8] A. Mellati, et al., Microengineered 3D cell-laden thermoresponsive hydrogels for mimicking cell morphology and orientation in cartilage tissue engineering, Biotechnol. Bioeng. 114 (2017) 217–231.
[9] F. Doberenz, K. Zeng, C. Willems, K. Zhang, T. Groth, Thermoresponsive polymers and their biomedical application in tissue engineering-A review, J. Mater. Chem. B 8 (2020) 607–628.
[10] X. Song, et al., Thermoresponsive hydrogel induced by dual supramolecular assemblies and its controlled release property for enhanced anticancer drug delivery, Biomacromolecules 21 (2020) 1516–1527.
[11] E. Bellotti, A.L. Schilling, S.R. Little, P. Decuzzi, Injectable thermoresponsive hydrogels as drug delivery system for the treatment of central nervous system disorders: a review, J. Control. Release 329 (2021) 16–35.
[12] C. Gong, et al., Thermosensitive polymeric hydrogels as drug delivery systems, Curr. Med. Chem. 20 (2013) 79–94.
[13] M. Liu, X. Song, Y. Wen, J.L. Zhu, J. Li, Injectable thermoresponsive hydrogel formed by alginate-g-poly(N-isopropylacrylamide) that releases doxorubicin-encapsulated micelles as a smart drug delivery system, ACS Appl. Mater. Interfaces 9 (2017) 35673–35682.
[14] R.C. op't Veld, et al., Thermosensitive biomimetic polyisocyanopeptide hydrogels may facilitate wound repair, Biomaterials 181 (2018) 392–401.
[15] L. Liu, et al., Thermo-responsive hydrogel-supported antibacterial material with persistent photocatalytic activity for continuous sterilization and wound healing, Compos. Part B Eng. 229 (2022), 109459.
[16] P. Makvandi, G.W. Ali, F. Della Sala, W.I. Abdel-Fattah, A. Borzacchiello, Biosynthesis and characterization of antibacterial thermosensitive hydrogels based on corn silk extract, hyaluronic acid and nanosilver for potential wound healing, Carbohydr. Polym. 223 (2019), 115023.
[17] L. Deng, et al., Magnetothermally responsive star-block copolymeric micelles for controlled drug delivery and enhanced thermo-chemotherapy, Nanoscale 7 (2015) 9655–9663.
[18] J. Bassi da Silva, P. Haddow, M.L. Bruschi, M.T. Cook, Thermoresponsive poly(di (ethylene glycol) methyl ether methacrylate)-ran-(polyethylene glycol methacrylate) graft copolymers exhibiting temperature-dependent rheology and self-assembly, J. Mol. Liq. 346 (2022), 117906.
[19] X.Z. Zhang, X.D. Xu, S.X. Cheng, R.X. Zhuo, Strategies to improve the response rate of thermosensitive PNIPAAm hydrogels, Soft Matter 4 (2008) 385–391.
[20] C.R. Becer, et al., Libraries of methacrylic acid and oligo(ethylene glycol) methacrylate copolymers with LCST behavior, J. Polym. Sci. Part A Polym. Chem. 46 (2008) 7138–7147.
[21] C. Pietsch, et al., Thermo-induced self-assembly of responsive poly(DMAEMA-b-DEGMA) block copolymers into multi- and unilamellar vesicles, Macromolecules 45 (2012) 9292–9302.
[22] A.H. Soeriyadi, et al., Synthesis and modification of thermoresponsive poly(oligo (ethylene glycol) methacrylate) via catalytic chain transfer polymerization and thiol-ene michael addition, Polym. Chem. 2 (2011) 815–822.
[23] D. Fournier, R. Hoogenboom, H.M.L. Thijs, R.M. Paulus, U.S. Schubert, Tunable pH- and temperature-sensitive copolymer libraries by reversible addition-fragmentation chain transfer copolymerizations of methacrylates, Macromolecules 40 (2007) 915–920.
[24] Q. Zhang, J.D. Hong, R. Hoogenboom, A triple thermoresponsive schizophrenic diblock copolymer, Polym. Chem. 4 (2013) 4322–4325.
[25] Q. Fang, T. Chen, Q. Zhong, J. Wang, Thermoresponsive polymers based on oligo (ethylene glycol) methyl ether methacrylate and modified substrates with thermosensitivity, Macromol. Res. 25 (2017) 206–213.
[26] A. Ramírez-Jiménez, K.A. Montoya-Villegas, A. Licea-Claverie, M.A. Gónzalez-Ayón, Tunable thermo-responsive copolymers from DEGMA and OEGMA synthesized by RAFT polymerization and the effect of the concentration and saline phosphate buffer on its phase transition, Polymers (Basel) 11 (2019).
[27] Q. Li, A.P. Constantinou, T.K. Georgiou, A library of thermoresponsive PEG-based methacrylate homopolymers: How do the molar mass and number of ethylene glycol groups affect the cloud point? J. Polym. Sci. 59 (2021) 230–239.
[28] J.F. Lutz, Thermo-switchable materials prepared using the OEGMA-platform, Adv. Mater. 23 (2011) 2237–2243.
[29] J.F. Lutz, Polymerization of oligo(ethylene glycol) (meth)acrylates: Toward new generations of smart biocompatible materials, J. Polym. Sci. Part A Polym. Chem. 46 (2008) 3459–3470.
[30] Z. Ye, et al., Molecular understanding of the LCST phase behaviour of P (MEO2MA-b-OEGMA) block copolymers, Mol. Simul. 47 (2021) 299–305.
[31] B. Kim, M. Kwon, A.K. Mohanty, H.Y. Cho, H. jong Paik, LCST and UCST transition of poly(DMAEMA-b-MEO2MA) copolymer in KHP buffer, Macromol. Chem. Phys. 222 (2021) 1–5.
[32] N.R. Rarokar, S.D. Saoji, P.B. Khedekar, Investigation of effectiveness of some extensively used polymers on thermoreversible properties of Pluronic® tri-block copolymers, J. Drug Deliv. Sci. Technol. 44 (2018) 220–230.
[33] A.P. Constantinou, et al., Investigation of the thermogelation of a promising biocompatible ABC triblock terpolymer and its comparison with pluronic F127, Macromolecules 55 (2022) 1783–1799.
[34] R. Hoogenboom, et al., Tuning the LCST of poly(2-oxazoline)s by varying composition and molecular weight: Alternatives to poly(N-isopropylacrylamide)? Chem. Commun. (2008) 5758–5760, https://doi.org/10.1039/b813140f.
[35] W. Webster, W.R. Herder, T.V. Rajanbabu, ref 11. 5300 (1983) 5706–5708.
[36] O.W. Webster, Group transfer polymerization: mechanism and comparison with other methods for controlled polymerization of acrylic monomers, Adv. Polym. Sci. 167 (2004) 1–34.
[37] O.W. Webster, Discovery and commercialization of group transfer polymerization, J. Polym. Sci. Part A Polym. Chem. 38 (2000) 2855–2860.
[38] K. Fuchise, Y. Chen, T. Satoh, T. Kakuchi, Recent progress in organocatalytic group transfer polymerization, Polym. Chem. 4 (2013) 4278–4291.
[39] F. Adams, P. Pahl, B. Rieger, Metal-catalyzed group-transfer polymerization: a versatile tool for tailor-made functional (co)polymers, Chem. - A Eur. J. 24 (2018) 509–518.
[40] Q. Li, L. Wang, F. Chen, A.P. Constantinou, T.K. Georgiou, Thermoresponsive oligo(ethylene glycol) methyl ether methacrylate based copolymers: composition and comonomer effect, Polym. Chem. 13 (2022) 2506–2518.
[41] I. Lilge, M. Steuber, D. Tranchida, E. Sperotto, H. Schönherr, Tailored (bio) interfaces via surface initiated polymerization: control of grafting density and new responsive diblock copolymer brushes, Macromol. Symp. 328 (2013) 64–72.
[42] B. Zhang, H. Tang, P. Wu, In depth analysis on the unusual multistep aggregation process of oligo(ethylene glycol) methacrylate-based polymers in water, Macromolecules 47 (2014) 4728–4737.
[43] Y. Li, et al., Synthesis, self-assembly, and thermosensitive properties of ethyl cellulose-g-P(PEGMA) amphiphilic copolymers, J. Polym. Sci. Part A Polym. Chem. 46 (2008) 6907–6915.
[44] L.T. Che, M. Hiorth, R. Hoogenboom, A.L. Kjøniksen, Complex temperature and concentration dependent self-assembly of poly(2-oxazoline) block copolymers, Polymers (Basel). 12 (2020) 1–16.
[45] X. Chang, D. Hu, L. Chen, Y. Wang, Y. Zhu, Synthesis, self-assembly and thermoresponsive behavior of Poly(lactide-co-glycolide)-b-Poly(ethylene glycol)-b-Poly(lactide-co-glycolide) copolymer in aqueous solution, Polymer (Guildf) 223 (2021), 123673.
[46] A.E. Smith, X. Xu, S.E. Kirkland-York, D.A. Savin, C.L. McCormick, 'Schizophrenic' self-assembly of block copolymers synthesized via aqueous RAFT polymerization: from micelles to vesicles, Macromolecules 43 (2010) 1210–1217.
[47] C.H. Ko, et al., Self-assembled micelles from thermoresponsive poly(methyl methacrylate)- b-poly(N-isopropylacrylamide) diblock copolymers in aqueous solution, Macromolecules 54 (2021) 384–397.

[48] H. Xiang, et al., Mechanical properties of biocompatible clay/P(MEO2MA-co-OEGMA) nanocomposite hydrogels, J. Mech. Behav. Biomed. Mater. 72 (2017) 74–81.
[49] A.C. Santos, et al., Phase diagrams of temperature-responsive copolymers p (MEO2MA-co-OEGMA) in water, Polymer (Guildf). 228 (2021).
[50] Copolymers, R. B. et al., Well-defined dual light- and thermo-responsive, 2020.
[51] A.L. Kjøniksen, M.T. Calejo, K. Zhu, B. Nyström, S.A. Sande, Stabilization of pluronic gels in the presence of different polysaccharides, J. Appl. Polym. Sci. 131 (2014) 1–8.
[52] A.P. Constantinou, T. Lan, D.R. Carroll, T.K. Georgiou, Tricomponent thermoresponsive polymers based on an amine-containing monomer with tuneable hydrophobicity: effect of composition, Eur. Polym. J. 130 (2020), 109655.
[53] S. Kasmi, et al., Transiently responsive block copolymer micelles based on N-(2-hydroxypropyl)methacrylamide engineered with hydrolyzable ethylcarbonate side chains, Biomacromolecules 17 (2016) 119–127.
[54] M. Serhan et al., Total iron measurement in human serum with a smartphone, in: AIChE Annu. Meet. Conf. Proc. 2019-Novem, 2019, pp. 1–11.
[55] H. Zhang, H. Xia, J. Wang, Y. Li, High intensity focused ultrasound-responsive release behavior of PLA-b-PEG copolymer micelles, J. Control. Release 139 (2009) 31–39.
[56] E.E. Brotherton, et al., Aldehyde-functional thermoresponsive diblock copolymer worm gels exhibit strong mucoadhesion, Chem. Sci. 13 (2022) 6888–6898.
[57] E. Raphael, M.J. Derry, M. Hippler, S.P. Armes, Tuning the properties of hydrogen-bonded block copolymer worm gels preparedviapolymerization-induced self-assembly, Chem. Sci. 12 (2021) 12082–12091.
[58] L.P.D. Ratcliffe, M.J. Derry, A. Ianiro, R. Tuinier, S.P. Armes, A single thermoresponsive diblock copolymer can form spheres, worms or vesicles in aqueous solution, Angew. Chemie - Int. Ed. 58 (2019) 18964–18970.
[59] Y. Gao, Z. Xiang, X. Zhao, G. Wang, C. Qi, Pickering emulsions stabilized by diblock copolymer worms prepared via reversible addition-fragmentation chain transfer aqueous dispersion polymerization: how does the stimulus sensitivity affect the rate of demulsification? Langmuir 37 (2021) 11695–11706.
[60] L.D. Blackman, K.E.B. Doncom, M.I. Gibson, R.K. O'Reilly, Comparison of photo- and thermally initiated polymerization-induced self-assembly: a lack of end group fidelity drives the formation of higher order morphologies, Polym. Chem. 8 (2017) 2860–2871.
[61] A. Shahrokhinia, R.A. Scanga, P. Biswas, J.F. Reuther, PhotoATRP-induced self-assembly (PhotoATR-PISA) enables simplified synthesis of responsive polymer nanoparticles in one-pot, Macromolecules 54 (2021) 1441–1451.
[62] A. Blanazs, et al., Sterilizable gels from thermoresponsive block copolymer worms, J. Am. Chem. Soc. 134 (2012) 9741–9748.
[63] N.J.W. Penfold, J.R. Whatley, S.P. Armes, Thermoreversible block copolymer worm gels using binary mixtures of PEG stabilizer blocks, Macromolecules 52 (2019) 1653–1662.
[64] X. Li, et al., Amphiphilic multiarm star block copolymer-based multifunctional unimolecular micelles for cancer targeted drug delivery and MR imaging, Biomaterials 32 (2011) 6595–6605.
[65] A.C. Santos, et al., Bulk dynamics of the thermoresponsive random copolymer of di(ethylene glycol) methyl ether methacrylate (MEO2MA) and oligo(ethylene glycol) methyl ether methacrylate (OEGMA), Polymer (Guildf) 148 (2018) 339–350.
[66] C. Zhang, et al., Conformation of hydrophobically modified thermoresponsive poly(OEGMA-co-TFEA) across the LCST revealed by NMR and molecular dynamics studies, Macromolecules 48 (2015) 3310–3317.
[67] A.C. Schmidt, H. Turgut, D. Le, A. Beloqui, G. Delaittre, Making the best of it: Nitroxide-mediated polymerization of methacrylates: via the copolymerization approach with functional styrenics, Polym. Chem. 11 (2020) 593–604.
[68] A.P. Constantinou, B. Zhan, T.K. Georgiou, Tuning the gelation of thermoresponsive gels based on triblock terpolymers, Macromolecules 54 (2021) 1943–1960.
[69] N. Badi, J.F. Lutz, PEG-based thermogels: applicability in physiological media, J. Control. Release 140 (2009) 224–229.
[70] N. Fechler, N. Badi, K. Schade, S. Pfeifer, J.F. Lutz, Thermogelation of PEG-based macromolecules of controlled architecture, Macromolecules 42 (2009) 33–36.
[71] P.Z. Elias, et al., A functionalized, injectable hydrogel for localized drug delivery with tunable thermosensitivity: synthesis and characterization of physical and toxicological properties, J. Control. Release 208 (2015) 76–84.
[72] I.B. Dicker, et al., Oxyanions catalyze group-transfer polymerization to give living polymers, Macromolecules 23 (1990) 4034–4041.
[73] S. Matsumura, et al., Stability and utility of pyridyl disulfide functionality in RAFT and conventional radical polymerizations, J. Polym. Sci. Part A Polym. Chem. 46 (2008) 7207–7224.
[74] V. Bütün, S.P. Armes, N.C. Billingham, Synthesis and aqueous solution properties of near-monodisperse tertiary amine methacrylate homopolymers and diblock copolymers, Polymer (Guildf) 42 (2001) 5993–6008.
[75] M.S. Kyriacou, S.C. Hadjiyannakou, M. Vamvakaki, C.S. Patrickios, Synthesis, characterization, and evaluation as emulsifiers of amphiphilic-ionizable aromatic methacrylate ABC triblock terpolymers, Macromolecules 37 (2004) 7181–7187.
[76] M.A. Ward, T.K. Georgiou, Thermoresponsive gels based on ABA triblock copolymers: Does the asymmetry matter? J. Polym. Sci. Part A Polym. Chem. 51 (2013) 2850–2859.
[77] V. Bütün, M. Vamvakaki, N.C. Billingham, S.P. Armes, Synthesis and aqueous solution properties of novel neutral/acidic block copolymers, Polymer (Guildf) 41 (2000) 3173–3182.
[78] P. Maksym-Bębenek, T. Biela, D. Neugebauer, Synthesis and investigation of monomodal hydroxy-functionalized PEG methacrylate based copolymers with high polymerization degrees. Modification by 'grafting from', React. Funct. Polym. 82 (2014) 33–40.
[79] A. Shrivastava, 2 – Polymerization, in: A.B.T.-I. Shrivastava to P. E., Plastics Design Library, William Andrew Publishing, 2018, pp. 17–48, doi: 10.1016/B978-0-323-39500-7.00002-2.
[80] R. Whitfield, et al., Tailoring polymer dispersity and shape of molecular weight distributions: methods and applications, Chem. Sci. 10 (2019) 8724–8734.
[81] A.P. Constantinou, L. Wang, S. Wang, T.K. Georgiou, Thermoresponsive block copolymers of increasing architecture complexity: a review on structure-property relationships, Polym. Chem. 14 (2023) 223–247.
[82] P. De, B.S. Sumerlin, Precision control of temperature response by copolymerization of di(Ethylene glycol) acrylate and an acrylamide comonomer, Macromol. Chem. Phys. 214 (2013) 272–279.
[85] M.A. Ward, T.K. Georgiou, Thermoresponsive triblock copolymers based on methacrylate monomers: effect of molecular weight and composition, Soft Matter 8 (2012) 2737–2745.
[88] N.K. Pandit, J. Kisaka, Loss of gelation ability of Pluronic® F127 in the presence of some salts, Int. J. Pharm. 145 (1996) 129–136.
[89] K.C. Shih, et al., What causes the anomalous aggregation in pluronic aqueous solutions? Soft Matter 14 (2018) 7653–7663.
[90] T. Li, T. Ci, L. Chen, L. Yu, J. Ding, Salt-induced reentrant hydrogel of poly (ethylene glycol)-poly(lactide-co- glycolide) block copolymers, Polym. Chem. 5 (2014) 979–991.
[91] A.P. Constantinou, N.F. Sam-Soon, D.R. Carroll, T.K. Georgiou, Thermoresponsive tetrablock terpolymers: effect of architecture and composition on gelling behavior, Macromolecules 51 (2018) 7019–7031.
[92] S.C. Sharma, et al., Viscoelastic wormlike micelles of long polyoxyethylene chain phytosterol with lipophilic nonionic surfactant in aqueous solution, J. Phys. Chem. B 113 (2009) 3043–3050.
[93] S.C. Sharma, L.K. Shrestha, K. Sakai, H. Sakai, M. Abe, Viscoelastic solution of long polyoxyethylene chain phytosterol/ monoglyceride/water systems, Colloid Polym. Sci. 288 (2010) 405–414.
[94] S. Bulut, J. Hamit, U. Olsson, T. Kato, On the concentration-induced growth of nonionic wormlike micelles, Eur. Phys. J. E 27 (2008) 261–273.
[95] T. Ahmed, K. Aramaki, Temperature sensitivity of wormlike micelles in poly (oxyethylene) surfactant solution: Importance of hydrophilic-group size, J. Colloid Interface Sci. 336 (2009) 335–344.
[96] T. Smart, et al., Block copolymer nanostructures, Nano Today 3 (2008) 38–46.
[97] T. Tang, et al., Thermo-responsive poly(methyl methacrylate)-block-poly(N-isopropylacrylamide) block copolymers synthesized by RAFT polymerization: micellization and gelation, Macromol. Chem. Phys. 207 (2006) 1718–1726.
[98] E. Hecht, K. Mortensen, M. Gradzielski, H. Hoffmann, Interaction of ABA block copolymers with ionic surfactants. Influence on micellization and gelation, J. Phys. Chem. 99 (1995) 4866–4874.
[99] S. Liu, et al., Synthesis and characterization of the Fe-substituted ZSM-22 zeolite catalyst with high n-dodecane isomerization performance, J. Catal. 330 (2015) 485–496.
[100] J.M. White, M.A. Calabrese, Impact of small molecule and reverse poloxamer addition on the micellization and gelation mechanisms of poloxamer hydrogels, Colloids Surfaces A Physicochem. Eng. Asp. 638 (2022), 128246.
[101] A. Kelarakis, et al., Association properties of a diblock copolymer of ethylene oxide and styrene oxide in aqueous solution studied by light scattering and rheometry, Macromol. Chem. Phys. 202 (2001) 1345–1354.
[102] C. Brunot, et al., Cytotoxicity of polyethyleneimine (PEI), precursor base layer of polyelectrolyte multilayer films, Biomaterials 28 (2007) 632–640.
[103] A.K. Pearce, R.K. O'Reilly, Polymers for biomedical applications: the importance of hydrophobicity in directing biological interactions and application efficacy, Biomacromolecules 22 (2021) 4459–4469.
[104] A.P. Constantinou, et al., Homo- and co-polymerisation of di(propylene glycol) methyl ether methacrylate – a new monomer, Polym. Chem. 12 (2021) 3522–3532.